Optimal experimental hyperspectral image acquisition conditions of biomedical structures

Rubaiya Hussain

Abstract—In recent decades there has been a great interest in using hyperspectral imaging (HSI) for biomedical applications. HSI provides a three dimensional dataset from which one can obtain both the spatial and spectral information of biological samples being imaged. From the acquired hyperspectral images, it is possible to extract diagnostic information about tissue constituents and morphology. This paper focuses on determining the experimental conditions for an optimal hyperspectral acquisition of biological samples.

Index Terms—Biomedical applications, diagnostic information, hyperspectral imaging, spectral curves, spatial resolution, tissue composition.

1 Introduction

Spectral imaging is imaging in several wavelength bands. The common RGB camera makes use of a filter that separates the light into three wavelengths- red, green, and blue. In multispectral imaging, the number of wavelength bands is about ten while in hyperspectral imaging, the number of distinct bands could be as high as several hundreds. Apart from a high number of wavelength bands, the hyperspectral camera can detect a higher wavelength range (200nm – 2500nm) and offers a wide range of applications in remote sensing, archaeology and art conservation, [1, 2] vegetation and water resource control [3,4], food quality and safety control [5,6] forensic medicine, [7,8] crime scene detection, [9,10] biomedicine [11,12] etc.

For biomedical applications, hyperspectral imaging shows great potential especially in the areas of disease diagnosis. The biological and pathological changes in tissues and organs have a close relationship with the spectra [13]. Thus different pathological conditions can be identified from the spectral information of each pixel in the hyperspectral images.

A hyperspectral imager mainly consists of a light source, a dispersive element (prism, grating, etc) and a 2D detector array. Such imagers use the 'push-broom' method to obtain hyperspectral data of a scene. This method captures a single line of spatial information containing full-spectrum data for every spatial pixel in the line [14]. In the basic design of a hyperspectral camera (Fig. 1), the light from the tissue sample passes through the entrance aperture of the camera and some other aberration correcting elements.

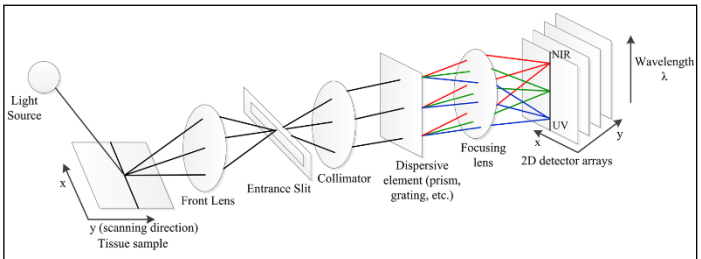

Fig.1: Schematic diagram of a hyperspectral imaging system [15].

The incoming light beam is then focused onto a slit by a focusing mirror which transforms it into a collimated beam and then focuses on a dispersive element (grating) that separates the beam into its different wavelength components. The dispersed light beam emerging from the grating is now passed through the lens optics system with the effect that for each pixel interval along the line defined by the slit (spatial axis), a corresponding spectrum is projected on a column of detectors on the array. The data read out from the array thus contains a slice of a hyperspectral image, with spectral information in one direction and spatial (image) information in the other. By scanning over the tissue sample, the camera collects slice from adjacent lines, forming a three dimensional data set called "hypercube" with two spatial dimensions and one spectral dimension [15]. This is illustrated in Fig. 2.

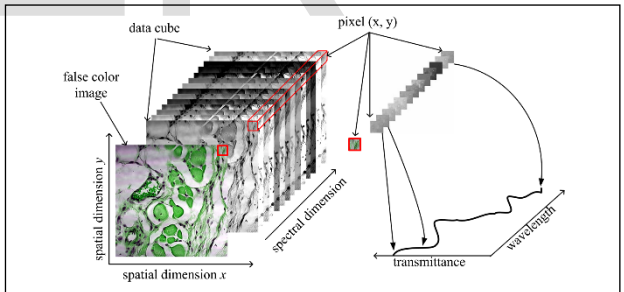

Fig. 2: Hyperspectral datacube showing two spatial dimensions (x and y) and one spectral dimension [13].

The main focus of this paper is to determine the conditions and specifications of the imaging system needed for an optimal hyperspectral acquisition of biological samples. For this purpose, a VNIR scientific CMOS camera and a photospectrometer has been used together with a transmissive light microscope to acquire hyperspectral images. The acquired hyperspectral images using varying amount of the intensity of the incident light, at different wavelength bands have been compared to that seen with the microscope eye-piece and also with that taken by another CCD camera. This allowed the determination of the amount of incident light needed to optimize the hyperspectral image acquisition process. Furthermore, the field of view, magnification, spatial and spectral resolutions of the hyperspectral imaging system have also been computed.

IJSER

2 MATERIALSAND METHODS

The experimental setup is shown in Fig. 3. The system consists of a photo-spectrometer SpecimV10 (SpecIm Ltd) connected to a high sensitivity sCMOS camera from PCO. The overall system is operative in the 400-1000 nm spectral range, with a spectral resolution of about 0.89nm. The hyperspectral camera system is coupled to an optical microscope, Nikon Eclipse TE 2000-U (see technical details in Fig. 4). The HSI system uses the Camware software for acquisition and visualisation of the images. The camera can also be controlled using this software. The user-friendly graphical interface can provide images at different chosen wavelengths and spectral graphs can be obtained for a particular selected position on the images.

In order to calculate the field of view of the hyperspectral camera system, a grating with known dimensions is imaged using the optical microscope coupled with the HSI system.

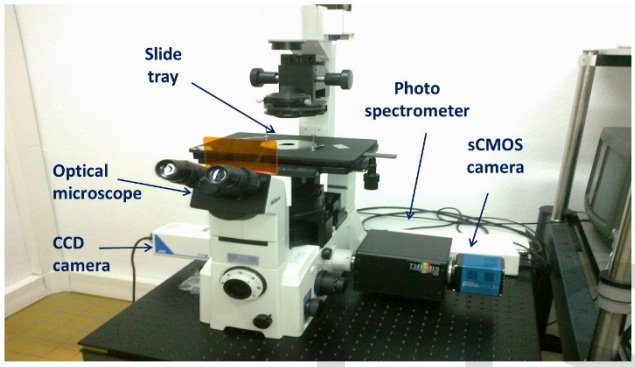

Fig. 3: Experimental setup of the hyperspectral imaging system.

Camera : pco.edge sCMOS		Spectrometer: SPECIM V10		Optical Microscope: Nikon Eclipse TE 2000-U	
Resolution	2560 x 2160 pixel	Spectral region	400-1000nm	Numerical aperture	1.05
Pixel size	6.5µm x 6.5 µm	F-number	F/ 2.8	Objective magnification	10 X
Full well capacity	30 000e⁻	Spectral sampling	0.63 – 5.0nm per pixel	Eye piece lens	10X (FOV 22mm)
Readout noise	<1.3rms	Spectral resolution	6.8nm	Tube magnification	1 or 1.5
Dynamic range	27000: 1 (88.6dB)	Spatial resolution	< 40 µm	Microscope configuration	Transmissive
Quantum efficiency	>54% @peak	Slit width	30µm x 14 µm		
Spectral range	370 nm – 1100nm	Lens mount	C-mount		
Frame rate	100fps				

Fig. 4: Technical specifications of the HSI system.

3 RESULTS AND DISCUSSION

3.1 Evaluation of the field of view and spatial resolution of the HSI system

The field of view has been evaluated by imaging a grating with known dimensions. On the grating, 100 lines equals to 10 mm. Therefore, for 1 line corresponds to 0.1mm.Number of vertical lines observed on the computer screen = 15 lines. Number of horizontal lines observed on the computer screen = 3 lines.

Estimated field of view = 1.5mm on the horizontal axis and 0.3mm on the vertical axis. Effective linear magnification of the camera = (size of the sensor used)/(field of view) = (2560 x 6.5um)/1.5mm = 11.

It has been mentioned before that the hyperspectral imaging system works as a scanner taking a slice of the image at a time. The different wavelength components of each slice are dispersed on the pixels along one of its axis. Thus, for each slice of the observed object, a 2D image is obtained with one spatial and one spectral axis. By taking the entire FOV, a 3D hypercube is formed with two of the dimensions being the spatial axis and the last being the spectral axis. The number of slices is fixed by setting the number of frames to capture on the hyperspectral camera. The maximum number of frames is 1000 which corresponds to the entire field of view along the scanning direction. Using this, the time to capture an entire field of view is calculated to be,

Capture time = number of frames ÷ frame rate = 500 ÷ 100fps = 5s.

The speed of the micro-translator needed to translate the specimen= (field of view in the scanning axis)/(capture time) = 1.5mm/5s = 0.3 mm/s.

Spatial resolution = (field of view in the scanning axis)/(number of pixels) = 1.5mm/2560 = 0.6µm.

It is noted that the resolution of the image is not diffraction limited but limited by the size of each pixel.For a diffraction limited system, the resolution should be,

$R_{diffraction}$ = 0.61 λ/ NA = 0.32 µm (assuming an incident light of wavelength 550nm).

The size of the diffraction resolvable unit projected on the sensors is about 3mm, using a magnification of 10. For the image seen on the sensor to be diffraction limited, using the Nyquist sampling theorem, the pixel size should be half of the resolvable unit. This corresponds to a pixel size of 1.5mm.

The spectral resolution is equal to the amount of dispersion for each pixel. This as seen on the technical documentation of the hyperspectral camera is equal to 0.89 nm.

3.2 Hyperspectral imaging of a mouse colon tissue:

The observed images of a biological tissue (colon slice of a mouse) at different wavelength bands acquired with the hyperspectral imaging camera are shown in Fig 5. The spectral curve shown in Fig.6(b) is obtained for different positions on the tissueas shown in Fig.6(a).

From the acquisitions of the tissue samples, it has been observed that at different wavelengths some features of a sample become easier to observe. Also due to the large amount of

spectral bands, a careful selection has to be made of bands which contained the most useful information about the specimen. Doing this in practice often depends on what application the scientist is interested in, for example an unusual cell in the midst of many identical cells. Image processing softwares are used to perform this selection based on different hyperspectral image processing methods [16,17].

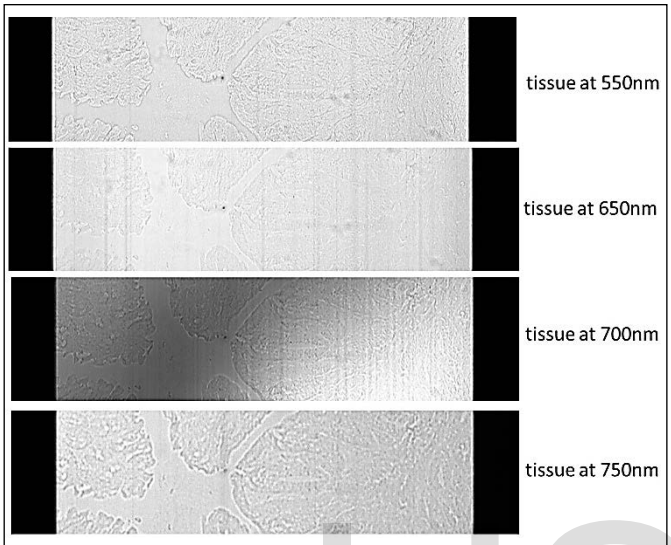

Fig. 5: Hyperspectral images of mouse colon tissue at different wavelengths acquired with the setup in Fig. 3.

The graph of the digital number against the wavelength in Fig. 6b) shows that for positions on the image (Fig 6a)) with similar constituents the spectral curves does not vary much compared to positions with a different constituent. This means that the hyperspectral imaging data can be used to characterize different constituents of the specimen being imaged.

From the acquisition of hyperspectral images, it has also been observed that the intensity of the incident light source is required to be increased compared to the level needed for conventional microscopy with a CCD camera. This is because in case of hyperspectral imaging, the light scattered by the object reaching the sensors is dispersed across several pixels in the spectral direction. This reduces the amount of light detected at each pixel location and explains the need for more sensitive cameras (e.gsCMOS or EMCCDs) for hyperspectral imaging.

4 Conclusion

The aim of this work has been to understand and determine the conditions for acquiring good hyperspectral images of biological samples. For this purpose, a VNIR sCMOS camera together with a photo-spectrometer has been used to form a hyperspectral imaging system. The field of view and the spatial resolution of the HSI system are then evaluated by using gratings of known dimensions which are imaged by coupling the HSI system with an optical microscope.

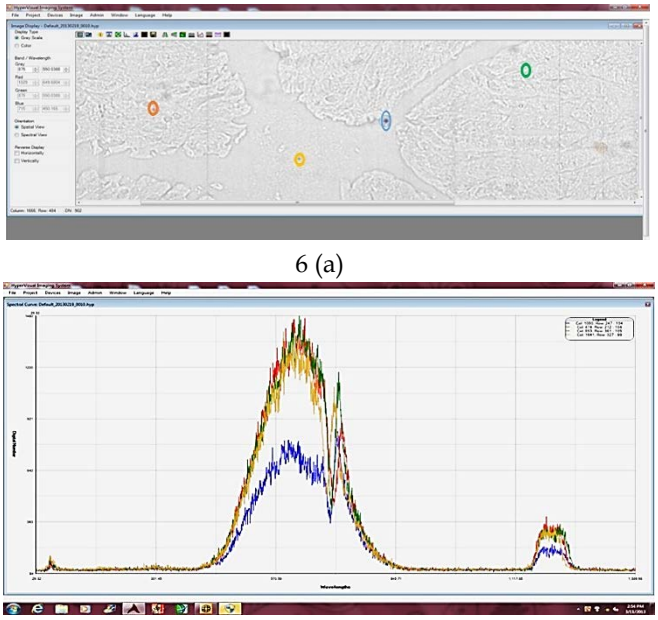

6 (a)

6 (b)

Fig. 6: (a) Observation of the tissue at different positions marked with circles. (b) Spectral curves of digital number versus wavelength at the positions marked in (a).

Then hyperspectral images of mouse colon tissues are acquired. From the images obtained it has been observed that certain features of the tissue samples are visible only at certain wavelength bands. However, due to the high number of spectral information available from an HSI system, the wavelength bands have to be selected carefully depending on the intended application. Spectral graphs of selected positions on the acquired images are then obtained. The regions with similar constituents showed no change in the spectral curves compared to those with a different constituent. Therefore, specimen constituents can be characterized by comparing the spectral curves at different locations. Thus, hyperspectral imaging can be used in obtaining information about tissue composition and shows much potential to be used in many other biomedical applications.

Acknowledgment

The author would like to thank Prof. Moulud Adel for his supervision and guidance during the project and JulieneSalvatier for providing the tissue samples used in the experiment. I would also like to thank Temitope Paul Onanuga for his immense help during the experiments.The experiments were carried out in Insitut Fresnel, Marseille, France.

References

[1] Fischer C, Kakoulli I., "Multispectral and hyperspectral imaging technologies in conservation: current research and potential applications," *Stud. Conserv.7*, 3 –16 (2006). 0039-3630

[2] Liang H, "Advances in multispectral and hyperspectral imaging for archaeology and art conservation," *Appl. Phys. A. 106, (2),* 309 –323

(2012). 0947-8396

[3] Govender M., Chetty K., Bulcock H., "A review of hyperspectral remote sensing and its application in vegetation and water resource studies," *Water SA. 33, (2)*, 145 –151 (2007). 0378-4738

[4] Adam E., Mutanga O., Rugege D., "Multispectral and hyperspectral remote sensing for identification and mapping of wetland vegetation: a review,"*Wetlands Ecol. Manage. 18, (3),* 281 –296 (2010). 0923-4861 CrossRef

[5] Gowen A. A. et al., "Hyperspectral imaging—an emerging process analytical tool for food quality and safety control," *Trends Food Sci. Technol. 18, (12), 590 –598 (2007)*. 0924-2244 CrossRef

[6] Feng Y. Z., Sun D. W., "Application of hyperspectral imaging in food safety inspection and control: a review," *Crit. Rev. Food Sci. Nutr. 52, (11)*, 1039 –1058 (2012). 0099-0248 CrossRef

[7] Edelman G. J. et al., "Hyperspectral imaging for non-contact analysis of forensic traces," *Forensic Sci. Int. 223, (1–3)*, 28 –39 (2012). 0379-0738 CrossRef

[8] Malkoff D. B., Oliver W. R., "Hyperspectral imaging applied to forensic medicine," *Proc. SPIE. 3920, 108 –116 (2000)*. 0277-786X CrossRef

[9] Kuula J. et al., "Using VIS/NIR and IR spectral cameras for detecting and separating crime scene details," *Proc. SPIE. 8359, 83590P (2012).* 0277-786X CrossRef

[10] Schuler R. L., Kish P. E., Plese C. A., "Preliminary observations on the ability of hyperspectral imaging to provide detection and visualization of bloodstain patterns on black fabrics," *J. Forensic Sci. 57, (6),* 1562 –1569 (2012). 0022-1198 CrossRef

[11] Carrasco O. et al., "Hyperspectral imaging applied to medical diagnoses and food safety," *Proc. SPIE. 5097, 215 –221 (2003).* 0277-786X CrossRef

[12] Afromowitz M. A. et al., "Multispectral imaging of burn wounds: a new clinical instrument for evaluating burn depth," *IEEE Trans. Biomed. Eng. 35, (10)*, 842 –850 (1988). 0018-9294 CrossRef

[13] Li Q, He X, Wang Y, Liu H, Xu D, Guo F; "Review of spectral imaging technology in biomedical engineering: achievements and challenges." *J.Biomed.Opt.0001;18(10):*100901-100901.

[14] Kim, M. S., et al. "Line-scan hyperspectral imaging platform for agro-food safety and quality evaluation: System enhancement and characterization."*Transactions of the ASABE 54.2 (2011):* 703-711.

[15] Lu, Guolan, and BaoweiFei. "Medical hyperspectral imaging: a review."*Journal of biomedical optics 19.1 (2014):* 010901-010901

[16] Du, Hongtao, et al. "Band selection using independent component analysis for hyperspectral image processing." *Applied Imagery Pattern Recognition Workshop, 2003. Proceedings. 32nd. IEEE, 2003.*

[17] Wang, Liguo, and Chunhui Zhao. Hyperspectral Image Processing. Springer, 2015.

IJSER